Applied Energy 395 (2025) 126205

Contents lists available at ScienceDirect

Applied Energy

journal homepage: www.elsevier.com/locate/apenergy

Integrated tidal power potential in the Seto Inland Sea in Japan with cost–benefit analysis

Morhaf Aljber [a,*], Han Soo Lee [a,b,c,**], Jae-Soon Jeong [b]

[a] Coastal Hazards and Energy System Science Laboratory, Graduate School of Innovation and Practice for Smart Society, Hiroshima University, 1-5-1 Kagamiyama, Higashi-Hiroshima, 739-8529 Hiroshima, Japan
[b] Center for Planetary Health and Innovation Science (PHIS), IDEC Institute, Hiroshima University, Japan
[c] Transdisciplinary Science and Engineering Program, Graduate School of Advanced Science and Engineering, Hiroshima University, Japan

HIGHLIGHTS

- The Seto Inland Sea possesses high potential for tidal power in Japan.
- Velocity variance among flood and ebb tide at optimal sites produces constant power.
- The average LCOE at the optimal sites is approximately (31–90) JPY/kWh.
- Annual generation of 374.64 GWh supplies more than 85,000 households.
- 166,000 tons per year reduction in CO_2 emission supports sustainable energy plans.

ARTICLE INFO

Keywords:
Tidal power competitiveness
Levelised cost of energy
Marine renewable price
Sustainable energy transition
LCOE
Carbone neutrality

ABSTRACT

Tidal power generation (TPG) provides a predictable and stable energy supply, making it a valuable complement to variable renewable sources such as solar and wind. However, its commercial viability remains constrained by high capital costs, complex installation requirements, and limited specialised infrastructure. This study assesses the economic feasibility of TPG in the Seto Inland Sea in Japan using the levelised cost of energy (LCOE) as a benchmark for competitiveness. The findings indicated that with a 10 % discount rate, the $LCOE_{ave}$ is approximately 85,990 ¥/MWh, whereas a 5 % discount rate reduces it to 31,088 ¥/MWh. The estimated annual energy production (AEP) was 374,640 MWh, sufficient to supply 89,735 households, with an equivalent CO_2 reduction of approximately 166,000 tons per year. Achieving cost competitiveness for TPGs requires large-scale deployment and supportive government incentives. Expanding infrastructure and leveraging economies of volume are crucial for reducing costs and enabling broader adoption. Despite existing challenges, TPG holds significant potential for enhancing Japan's energy security and contributing to its decarbonisation goals. This potential depends on effective grid integration, strong policy support, and sustained strategic investment.

1. Background

1.1. Introduction

Global commitments to climate change adaptation and mitigation have intensified the deployment of renewable energy. Numerous countries have established ambitious targets for reducing greenhouse gas (GHG) emissions [1]. The feasibility of renewable energy completely replacing conventional thermal energy sources has emerged as a prominent research field [2–4]. Several studies have outlined strategies to achieve national energy systems powered entirely by renewable sources [5–9]. These studies are increasingly supported by real-world achievements, with some nations reporting consecutive days powered solely by renewable energy [10,11]. Such milestones underscore the potential for achieving carbon neutrality. Consequently, maximising the exploitation of all renewable energy sources has become imperative.

* Corresponding author at: Coastal Hazards and Energy System Science Laboratory, Graduate School of Innovation and Practice for Smart Society, Hiroshima University, 1-5-1 Kagamiyama, Higashi-Hiroshima, 739-8529 Hiroshima, Japan.
** Corresponding author at: Center for Planetary Health and Innovation Science (PHIS), IDEC Institute, Hiroshima University, Japan.
E-mail addresses: d232882@hiroshima-u.ac.jp (M. Aljber), leehs@hiroshima-u.ac.jp (H.S. Lee).

https://doi.org/10.1016/j.apenergy.2025.126205
Received 19 February 2025; Received in revised form 4 May 2025; Accepted 23 May 2025
Available online 31 May 2025
0306-2619/© 2025 The Authors. Published by Elsevier Ltd. This is an open access article under the CC BY-NC license (http://creativecommons.org/licenses/by-nc/4.0/).

Marine renewable energy (MRE) is particularly notable for its distinct advantages, including minimal land use and access to abundant and predictable energy resources [12–14]. Offshore wind power experienced rapid growth due to successful implementation and strong governmental support. This growth has reduced industry risk, driving down energy costs and attracting global investment [15,16]. Additionally, financial incentives such as subsidies have encouraged developers to invest in large-scale offshore wind projects [15,17,18]. These efforts have collectively lowered the energy cost and facilitated the global adoption of offshore wind power [19].

Tidal power generation (TPG) is another promising source of MREs. Unlike wind and solar energy, tidal currents are predictable over extended periods, a crucial characteristic for accurate grid supply management [20–22]. Many countries possess tidal power potential, making TPGs valuable components in mixed offshore power systems for stabilising and balancing energy production [23,24]. Decades of research and pilot projects have propelled the TPG from a fledgling stage to active implementation [25]. As a result, countries have begun the integration of TPGs into their renewable energy portfolios [26–28]. The MeyGen tidal site phase A1 in the UK published valuable knowledge regarding manufacturing, deployment, and project management [29]. With progressive development and information sharing, the learning rate is rapidly increasing and spreading, which results in greater cost reduction [30]. This collaboration has already been observed at the Goto tidal site in Japan, where the cost was lower than that of the first deployment at the MeyGen tidal site in the UK [31].

The cost of tidal energy or levelised cost of energy (LCOE) remains inadequately addressed because active tidal sites operate with a small number of turbines [29]. Studies have proposed methodologies that integrate both cost and flow parameters to estimate the LCOE [32]. Other studies have suggested that increasing the installed capacity potentially decreases the LCOE [33]. Moreover, combining multiple MREs, such as tidal and wave power, reduces the overall grid connection costs. In some cases, pilot tidal turbine models have been employed to estimate LCOE by incorporating field or numerical test results, where cost inputs are provided directly by developers [34,35]. However, these assessments often overlook site-specific geographical constraints. Many tidal straits serve as key navigational routes or support fishing and recreational activities. Therefore, LCOE estimations should consider only the areas available for turbine deployment within each site. Scaling up to larger tidal farms with multiple turbines is essential for achieving economic power production. However, deploying tidal turbines poses greater challenges, as they require specialised teams and equipment, significantly increasing project expenditures [34,36]. Innovative approaches, such as floating tidal turbines, have been developed to circumvent subsea construction and reduce costs [35,37]. The cost reduction potential is also evident from learning curves in tidal energy deployment. For example, a report by Arup [38] estimated that doubling the installed tidal capacity could reduce capital expenditures (CAPEX) by 13 % and operational expenditures (OPEX) by 19 %. Similarly, a 13 % CAPEX reduction but a lower OPEX reduction of 11 % was projected [39]. These insights highlight the importance of scaling and innovation in advancing the economic viability of TPGs.

The deployment of renewable energy in Japan has increased over 24 % by 2021 [40]. In 2019, the first tidal pilot project was launched offshore of Nagasaki Prefecture in the Goto Archipelago. The 500-kW tidal turbine entered the commissioning phase in 2021 to export approximately 242 MWh of accumulated energy production in 8 months [31]. Another tidal turbine with a capacity of 1.1 MW was installed to increase the farm capacity [41]. Owing to the difference in tidal harmonic phases between sites in western Japan, uninterrupted power production could be reached [42]. A single tidal farm is insufficient, as the LCOE might soar. However, the full exploitation of Japanese national water provides a sustainable source of renewable energy.

The Seto Inland Sea (SIS) in the western part of Japan holds high potential for TPGs. A tidal current velocity above 2 m/s is common in several straits [43]. To identify the optimal locations for the TPG in the SIS, a multicriteria decision-making-based GIS analysis was used, and the optimal locations were identified in the Naruto Strait, Akashi Strait, Matsushima Island, Shimanami Islands, Kurushima Strait, Tsuwaji Strait, and Obatake Strait [44,45].

In this study, we aim to establish a threshold for LCOE and provide a baseline for TPG prospects in Japan on the basis of tidal power production from optimal locations in the SIS. The LCOE is the energy price that a tidal farm must receive to be economically effective and is a critical proxy for determining the feasibility of the TPG over other MREs in Japan [46]. The LCOE is susceptible to the available subsidies, especially at the early stage of tidal farm deployment. Since an assumption is unnecessary, the LCOE is less uncertain and robust for feasibility assessment [47]. In Aljber et al. [44], the annual energy production (AEP) and the equivalent CO_2 reduction were calculated at one optimal location. However, holistic tidal power production from all optimal locations in the SIS was not provided. Furthermore, there was no economic analysis of the TPG.

Four tidal farms are proposed in this study, and the AEP is calculated for each farm and used to calculate the LCOE. The combined AEP from all tidal farms is subsequently used to calculate the number of households that dispensed clean energy and the equivalent CO_2 reduction. The resulting LCOE, however, is not final and has some uncertainty due to the resolution of the tidal current model [44,48,49]. Furthermore, the wake effect was not considered in this study.

This paper is structured as follows: In the first section, the introduction and description of tidal site selection and readiness are provided. Section 2 describes the methods that involve tidal turbine candidates for the optimal sites in the SIS, tidal power, and LCOE calculations. The results are presented in the third section. Section 4 presents the discussion, and the conclusion is presented in Section 5.

1.2. Tidal site selection and preparedness

The SIS is the largest semi-enclosed water body in western Japan, with an approximate area of 23,000 km^2 and a length of approximately 500 km [50]. The SIS has been recognised for TPG development due to its high current velocity [42,51]. An approach was taken to identify the optimal locations for TPGs in the SIS considering multiple constraints along with tidal velocity and water depth [44]. Ports and harbours exclusive zones and natural conservations were excluded from the selection. The water depth was considered only between 10 m and 100 m to circumvent shallow and deep locations [52]. The constraints were divided into two groups, the distance proximity, which encompassed distances from infrastructures such as ports, power stations, and densely populated regions. The second group included waves and nautical routes. Areas with high waves were eluded because they impinge on the installation and maintenance of tidal turbines [53]. A previous study suggested that tidal turbines typically operate safely under a significant wave height of 3 m or less [54]. Beyond this threshold, turbines often require shutdown to prevent fatigue. In terms of energy output, Lewis et al. [55] reported that each 1-m increase in wave height can lead to an approximate 10 % reduction in theoretical power. The wave loading tolerance varies depending on factors such as turbine size and installation depth. In the Seto Inland Sea (SIS), wave heights are generally low, approximately 0.4 m [44], due to the sea's semi-enclosed geography and the presence of numerous islands [50]. Frequent nautical routes were also eluded to avoid conflicts of interest between marine users [53]. Fig. 1 illustrates the proposed tidal sites among the optimal locations along with the administrative borders of the surrounding regions.

Compared with UK tidal sites, TPGs in Japan face a scarcity of logistical support. The commissioning and decommissioning require fully equipped ports [56]. Furthermore, the absence of large-scale manufacturing and supply chains for TPG systems drives up the cost. The need for specialised teams is evident when considering MRE. A recent offshore wind auction in Japan necessitated that for future

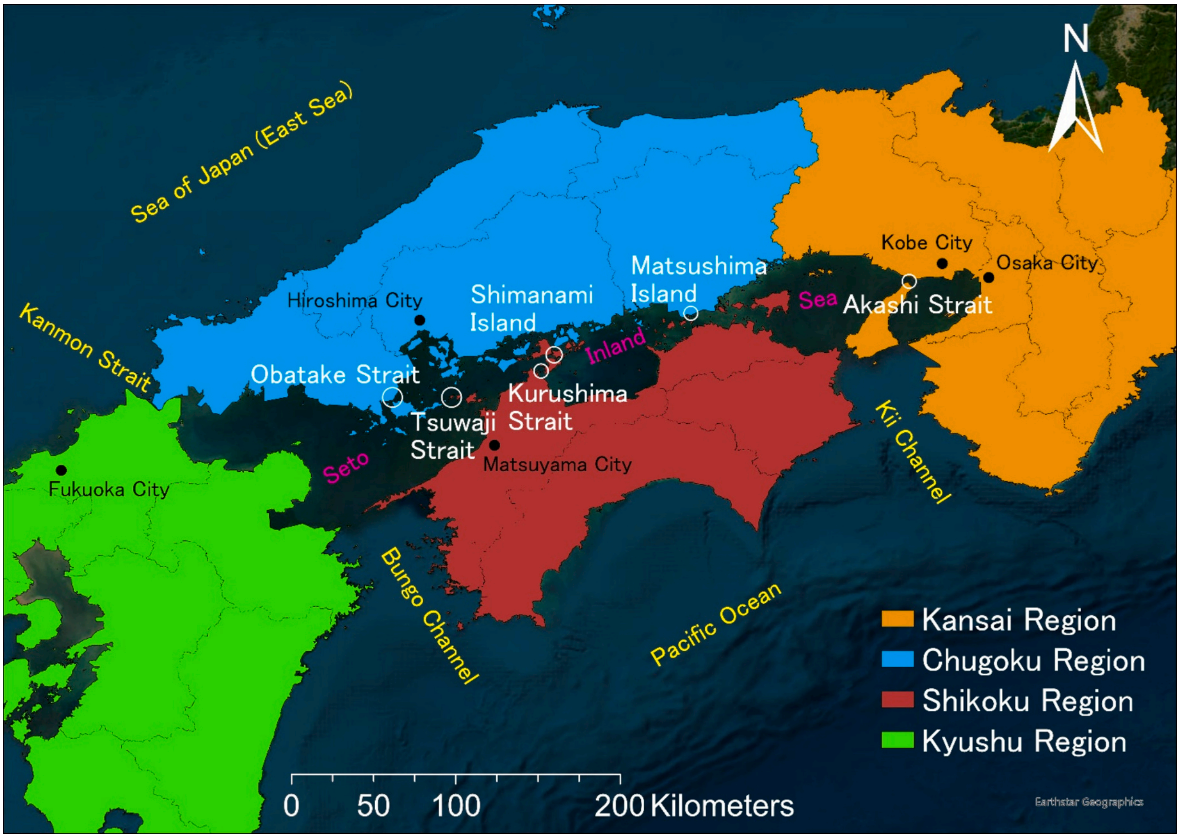

Fig. 1. The Seto Inland Sea and the surrounding administrative borders, with selected tidal sites: Akashi Strait, Matsushima Island, Shimanami Islands, Obatake Strait, Kurushima Strait, and Tsuwaji Strait.

expansion, designated ports must be equipped for construction and maintenance [57]. For TPGs, dedicated vessels, barges and self-elevated platforms are necessary [58]. These scarcities increase the CAPEX and OPEX, thereby increasing the LCOE. In contrast, other countries with TPG initiatives, such as France, possess tidal potential of up to 5.1 GW at sites such as Raz Blanchard and Alderney Race, which have fewer technical constraints and mature infrastructure [59]. However, a lack of a formal revenue support mechanism has hindered commercial expansion. In Canada, the Bay of Fundy has attracted several investors, such as Nova Innovation [60]. Promising sites such as the Minas Passage or Johnstone Strait on the east coast of Vancouver Island have some of the world's strongest tidal currents. However, slow regulatory processes and environmental monitoring requirements have delayed deployment [61,62]. In China, interest in TPGs is growing, with robust institutional support. However, many TPG projects remain in the demonstration phase due to technical challenges and high LCOE [63,64]. Japanese tidal sites are located near populated areas and nearshores, which facilitate direct connections and reduce cabling prices [65]. Unlike UK tidal sites, communication, electrical substations, and internet access are available [29]. Therefore, social and economic benefits could be brought to several small towns and islands in the SIS.

2. Method

2.1. Tidal turbine selection

Tidal turbine selection is based on three main constraints: the cut-in velocity, the rated velocity, and the water depth. Generally, the cut-in velocity is 0.5 m/s for small-scale tidal turbines with diameters less than 10 m and 1 m/s for those with greater diameters. The rated velocity ranges between 2 m/s and 4 m/s depending on the converter and gearbox. Table 1 shows some of the commercial tidal turbines that are in operation at the time of the draughting of this paper. For the water depth, at least 5 m of clearance must be preserved above and below the turbine blades to prevent the device from colliding with marine debris or bottom sediment [52].

The SIS has an average depth of 38 m [50]. Large ports and industrial cities are experiencing active shipping movements. Therefore, the

Table 1
Proposed commercial tidal turbines for tidal farms in the Seto Inland Sea with specifications for each turbine.

Turbine	Design	Cut-in velocity (m/s)	Rated power (kW)	Rated velocity (m/s)	Power coefficient (Cp)	Diameter (m)	Reference
SAE Renewables	Bottom fixed	1	500–2000	2–3	0.45	10–20	[42,89]
Nova M 100	Bottom foxed	0.5	100	2	0.42	9	[42,90]
Bluenergy	Floating	0.5	(7 × 4)	2.5	0.4	2	[86]
Orbital O2	Floating	1	(1000 × 2)	2.5	0.4	22	[91]
Magallanes ATIR	Floating	1	(1000 × 2)	2.9	0.5	19–21	[35,92]
Andritz-Hydro HS	Bottom fixed	1	500–2000	2–3	0.4	18–21	[93]
Sabella D10	Bottom fixed	0.5	1000	3–4	0.38	10	[27,94]
RivGen	Truss	0.5	50–80	2.25–3.5	0.4	~	[95–97]

optimal locations were identified in the vicinity of the high tidal velocity zones [44]. Tidal currents have high spatial variability in the horizontal direction, and a high resolution of 50 m or more is needed to select the installation location. Since the purpose of this study is feasibility assessment, the tidal farm design and calculation are based on the available high tidal velocity at optimal sites at a 100 m spatial resolution.

The tidal turbine SAE Renewables is considered for all tidal sites because it offers a range of diameters and rated velocities that are currently operating in the UK and Japan [29,66]. Moreover, the mentioned tidal sites in Japan and the UK have already published project budgets, which facilitate the calculation of LCOE.

2.2. Tidal power calculation

The tidal current velocity in the SIS was obtained from a high-resolution coastal and ocean circulation model by Jeong et al. [67]. The semi-implicit cross-scale hydroscience integrated system (SCHISM) model was used for the numerical simulation. SCHISM is a 3D ocean model based on the hydrostatic Navier–Stokes equations and a semi-implicit finite-element/volume method. The model was built with unstructured grids, and the spatial resolution ranged between approximately 30 m in upstream rivers and approximately 7000 m at the Pacific Ocean boundary. Thirty vertical layers were used, and an 80 s timestep was used. The simulation period considered was 56 days between August 12th and October 7th, 2011. For the feasibility assessment, the European Marine Energy Centre Ltd. [52] recommended a minimum tidal current simulation period of 30 days to capture the full monthly tidal cycle under normal conditions. The simulation period in this study overlaps with the typhoon season in the SIS. Therefore, the period was extended beyond 30 days to accommodate tidal velocity variation. For detailed explanations of the coastal and ocean circulation models, modelling results, validations, and applications for hazardous events, refer to [43,44,67]. The power output was calculated as follows:

The power for each turbine is as follows:

$$P = \frac{1}{2}\rho C_p A_{turbine} U_d^3 \tag{1}$$

The power per farm P_f is as follows:

$$P_f = P \times n_t \tag{2}$$

where ρ is the seawater density (1024 kg/m^3), C_p is the power coefficient (0.4), $A_{turbine}$ is the swept area of the turbine, U_d is the dominant tidal current velocity (the velocity in the dominant flow direction within the tidal site), and n_t is the number of turbines on the farm. To identify U_d, a harmonic analysis was performed at each tidal site via the U-tide function in Python. Then, the elliptical orientation of the M2 tide was analysed. The major axis angle of the M2 tide was extracted, and the velocity field was projected in the dominant direction. The absolute value of the dominant velocity U_d was then used for power calculations. Some tidal sites in the SIS are unidirectional and dominated by flood or ebb tides. Therefore, the direction with the highest velocity was used for accurate power estimation.

The annual energy production (*AEP*) is as follows:

$$AEP = 8760 \times \overline{C_{av}} \times P_f \tag{3}$$

where $\overline{C_{av}}$ is the coefficient of availability. It is the percentile of hours per day when the tidal current velocity exceeds the cut-in velocity of the tidal turbine. For each site, the number of hours when the tidal velocity $V \geq 1m/s$ was calculated for six days, three days during the spring tide and three days during the ebb tide. The selection of the days was to accommodate the highest and lowest tidal velocities during the peak spring and neap tides. The average number of hours for six days was subsequently calculated and used to obtain $\overline{C_{av}}$.

The AEP from all tidal farms was summed and used to calculate the number of households supplied with electricity (N) and the carbon dioxide reduction per year (R_c) as follows:

$$N = AEP/AAECH \tag{4}$$

$$R_c = N \times ACDEH \tag{5}$$

where AAECH is the average annual electricity consumption per household (4175 kWh/year), and ACDEH is the average annual carbon dioxide emission from electricity per household (1.85 ton-CO_2/year), obtained from a report published by the Ministry of Environment [68].

2.3. Levelised cost of energy (LCOE)

The LCOE is the most practically used metric to optimise and compare several types of energy [69]. The LCOE is a proxy used to determine the cost incurred by the developer to acquire and dispatch electricity. The LCOE is the proportion between the cost and the output energy, which is calculated as follows:

$$LCOE = \frac{Cost}{Energy} = \frac{CAPEX \times P_f + \sum_{i=1}^{L} OPEX_i \times P_f \times (1+r)^{-i}}{\sum_{i=1}^{L} AEP_i \times (1+r)^{-i}} \tag{6}$$

The CAPEX is paid once at the commencement of the tidal project, and it encompasses the turbines price, cabling, vessel time, and so on. The OPEX is paid annually, and it includes scheduled and unscheduled maintenance, environmental impact assessment, and operation. P_f is the power per farm in MW and AEP is calculated annually in MWh/year. r is the discount rate, and the project lifetime was proposed to be 25 years.

Three scenarios were considered for the LCOE calculation.

Scenario (I) uses Japanese market prices. A feasibility assessment report was published by NEDO [56] and suggested that CAPEX should be 565,000 ¥/kW. This assumption was adopted since it is close to the Goto tidal site budget [66]. The OPEX was not mentioned in previous reports. However, after calculating the proportion of the $OPEX/CAPEX$ in several studies, including the MeyGen report, it was found that the OPEX ranges from 3 to 5 % of the CAPEX [69–72]. Thus, the OPEX was considered to be 4 % of the CAPEX, and it is 22,600 ¥/kW.

Scenario (II) uses MeyGen prices. The CAPEX was £51.3 m, and the OPEX was £1.4 m per 6 MW rated power [29]. These prices were converted to the JPY using the exchange rate between the GBP and JPY as of 2019 before the COVID-19 pandemic (1 GBP equal to 140 JPY). Thus, CAPEX is 1,197,000 ¥/kW, and OPEX is 32,620 ¥/kW.

Scenario (III) uses the UK market price assumption after converting to the JPY via the same postulation as in the second scenario [47,73]. The third scenario includes the number of turbines in each farm in the calculation, which is a vital factor for turbine selection. Since tidal turbines are expensive to build and install, having a smaller array with large-scale turbines is beneficial. Therefore, the assumption was as follows:

$$\begin{aligned} \text{CAPEX} &= CA_f + CA_t \times n_t = £\,5.6\,m + £\,2.4\,m \times n_t \\ &= ¥\,784\,m + ¥\,336\,m \times n_t \end{aligned} \tag{7}$$

$$\begin{aligned} \text{OPEX} &= OP_f + OP_t \times n_t = £\,0.27\,m + £\,0.094\,m \times n_t \\ &= ¥\,37.8\,m + ¥\,13.16\,m \times n_t \end{aligned} \tag{8}$$

where CA_f and OP_f are the fixed CAPEX and OPEX (vessels, cables, foundation, installation, fixed maintenance, etc.), CA_t and OP_t are the costs that increase with the number of turbines, and n_t is the number of turbines.

LCOE is heavily affected by the discount rate, and since the discount rate represents technology risk and accountability, two discount rates are considered: pessimistic (10 %) and optimistic (5 %) [19].

3. Results

3.1. Gross tidal power production

The optimal TPG sites in the SIS were divided into four tidal farms on the basis of three criteria:

- Regional grouping – Sites within the same administrative region (Chugoku, Kansai, Shikoku, and Kyushu) were grouped together (Fig. 1).
- LCOE balance – If multiple sites were located in one region, they were split into two groups to ensure a balanced LCOE.
- Site proximity – The distance between sites was considered for efficient deployment.

Among the optimal locations, those with limited areas for installation or limited frequent high tidal current velocities were excluded. The four proposed tidal farms are (I) Akashi (Kansai region); (II) Matsushima + Obatake (Chugoku region); (III) Shimanami Islands (Shikoku region); and (IV) Kurushima + Tsuwaji (Shikoku region) (Fig. 2). The values in the legends of Fig. 2 are the rankings of the optimal sites, indicating that three is the best. The resolution of the tidal sites is 100 × 100 m. The turbines are aligned facing the dominant flow direction. This alignment is to maximise energy capture. The recommended spacing between turbines is 2.5 times the turbine diameter and 10 times the diameter between rows [52]. However, site-specific conditions influence these distances according to simulation and measurement results [74,75]. Since the simulation is outside the framework of this study, two placement strategies were adopted: (1) for turbine diameters close to 20 m, each cell accommodates one turbine, and (2) for diameters near 10 m, each cell accommodates two turbines. A cut-in velocity of $V_c = 1\ m/s$ was adopted for all turbines.

3.2. Akashi strait

The Akashi Strait is a vital passage connecting Osaka Bay with the inner part of the SIS in Harima Nada (Nada means basin in Japanese [50]). The two proposed tidal sites (Ak1 and Ak2) are located near Awaji Island (Fig. 2a). Ak1 has an average depth of 29 m, and the highest current velocity is 2.5 m/s. The selected diameter (D) was 18 m, and the rated velocity was $V_r = 2.3\ m/s$. The turbine hub height was −15 m. Ak1 had 15 cells and could accommodate 15 turbines. To calculate $\overline{C_{av}}$, the number of hours when the tidal current velocity exceeded V_c was extracted during the spring tide on Aug 29th = 12 h; Sep 13th = 11 h; Sep 29th = 12 h; and during the neap tide on Aug 20th = 5 h; Sep 6th = 5 h; Sep 23rd = 5.66 h. The mean hours for the six days were 8.44 h, and $\overline{C_{av}} = 0.35\%$.

Ak2 has an average depth of 35 m, and the highest current velocity is 2.36 m/s. The selected D was 20 m, $V_r = 2\ m/s$, and the turbine hub height was −15 m. The number of turbines was 9, the mean hours for the six days was 9.2 h, and $\overline{C_{av}} = 0.39\%$. Table 2 shows the site specifications for all tidal farms in the SIS.

A harmonic analysis was conducted to extract the dominant flow velocity. The elliptical orientation of the M2 tide is illustrated in Fig. 2a, and the major angle for M2 tides is Ak1 = 83.13° and Ak2 = 134.017°. Using the major angle, the dominant velocity was projected in the Y direction. Then, the absolute value of the dominant velocity was used to construct the occurrence likelihood. The occurrence likelihood presents the distribution of the tidal current and the frequency of occurrence of the tidal current velocity. The boxplot shows the range of the tidal current velocity between the minimum and maximum values, the weight of the distribution, and the median tidal velocity at the location. The left edge of the box is the first quartile, which is greater than 25 % of the data within the box. The red line inside the notch is the median, which is 50 % of the data. The right edge of the box is greater than 75 % of the data. The two whiskers extending from the edges represent the range of the data between the maximum and minimum values. Finally, the power was calculated via Eq. (1). Fig. 3 depicts the results for sites Ak1 and Ak2.

The power per site for Ak1 was $P_{fAk1} = 643 \times 15 = 9.645\ MW$, and that for Ak2 was $P_{fAk2} = 516 \times 9 = 4.644\ MW$. Hence, the power per farm was $P_f = 14.3\ MW$, and $AEP_{Ak1} = 29.6$ GWh/year and $AEP_{Ak2} = 15.86$ GWh/year. Hence, the AEP from Akashi Farm was 45.44 GWh/year. Using Eq. (6), the LCOE from the Akashi tidal farm was calculated. Table 3 shows the LCOE for all tidal farms. For the Akashi tidal farm, the LCOE for the Japanese market was approximately 84,000 ¥/MWh for a 10 % discount rate, and it dropped to approximately 31,000 ¥/MWh for a 5 % discount rate. The UK market assumption was similar to that of the Japanese market case. However, the MeyGen prices were the highest, with approximately 173,000 ¥/MWh for 10 % and approximately 61,000 ¥/MWh for the 5 % discount rate. The MeyGen project represents the first commissioned tidal farm with four turbines, resulting in high initial costs and elevated prices. Insights gained from MeyGen have contributed to significant cost reductions, as demonstrated at the Goto tidal site. MeyGen prices are essential, as they represent the most uncertain case with high CAPEX and OPEX.

3.3. Matsushima Island and the obatake strait

Matsushima Island is situated in the Bisan Strait, which connects Harima Nada to the middle part of the SIS in Hiuchi Nada. Two sites (Ma1 and Ma2) were identified near the island close to the Shimotsui-Seto Bridge (Fig. 2b). The Obatake Strait is in Yamaguchi Prefecture, and it connects Hiroshima Bay with Iyo Nada.

The dominant velocities for the two sites on Matsushima Island were projected in the Y and X directions following the major angle (Ma1 = 118.23° and Ma2 = 169.11°). The dominant velocity in the Obatake Strait was projected in the X direction following the major angle of 6.58°. Table 2 shows the specifications of the sites. The likelihood of occurrence and tidal power for Matsushima Island were subsequently calculated (Fig. 4). The power per site from Ma1 and Ma2 was $P_{fMa1} = 330 \times 2 = 0.66\ MW$ and $P_{fMa2} = 640.54 \times 7 = 4.5\ MW$, respectively. $AEP_{Ma1} = 2.3$ GWh/year, and $AEP_{Ma2} = 23.6$ GWh/year. From the Obatake Strait, the power per site was $P_{fob} = 7MW$, and $AEP_{ob} = 47\ GWh/year$ [44]. Thus, the total power per farm from the three sits was $P_f = 12.16\ MW$, and $AEP = 73\ GWh/year$. For LCOE, the optimum scenario was the third scenario with the UK market assumption since the number of turbines was small and the AEP was large. The LCOE was 44,320 ¥/MWh for the 10 % discount rate and 16,440 ¥/MWh for the 5 % discount rate. Japan's market prices were close to those in the third scenario. Owing to the large AEP, the MeyGen price was lower than that in the Akashi Strait, especially with a 5 % discount rate (Table 3), and the LCOE was 32,450 ¥/MWh. Although the two tidal farms, Matsushima Island and the Obatake Strait, are distant, both farms are located within the Chugoku region. Furthermore, both locations are far from the active shipping routes, especially the Obatake Strait, and they could contribute generously to the TPG due to their energetic tidal currents.

3.4. Shimanami Islands

The Shimanami Islands are a small archipelago located between Hiuchi Nada and Aki Nada. The archipelago consists of connected islands that form a popular tourist cycling destination from Honshu Island until Shikoku Island. High tidal current flows across the straits that develop within the archipelago. Three locations were identified as optimal for the TPG: the Hanaguri Strait, the Funaori Strait, and two sites near Taizaki Island (Fig. 2c). Table 2 lists the specifications for the four sites. The major angles were 46.23°, 18.12°, 130.55°, and 25.54° for the Hanaguri strait SH1, Funaori strait SF1, Taizaki Island ST1, and ST2, respectively. SH1 site accommodates only one turbine. The four

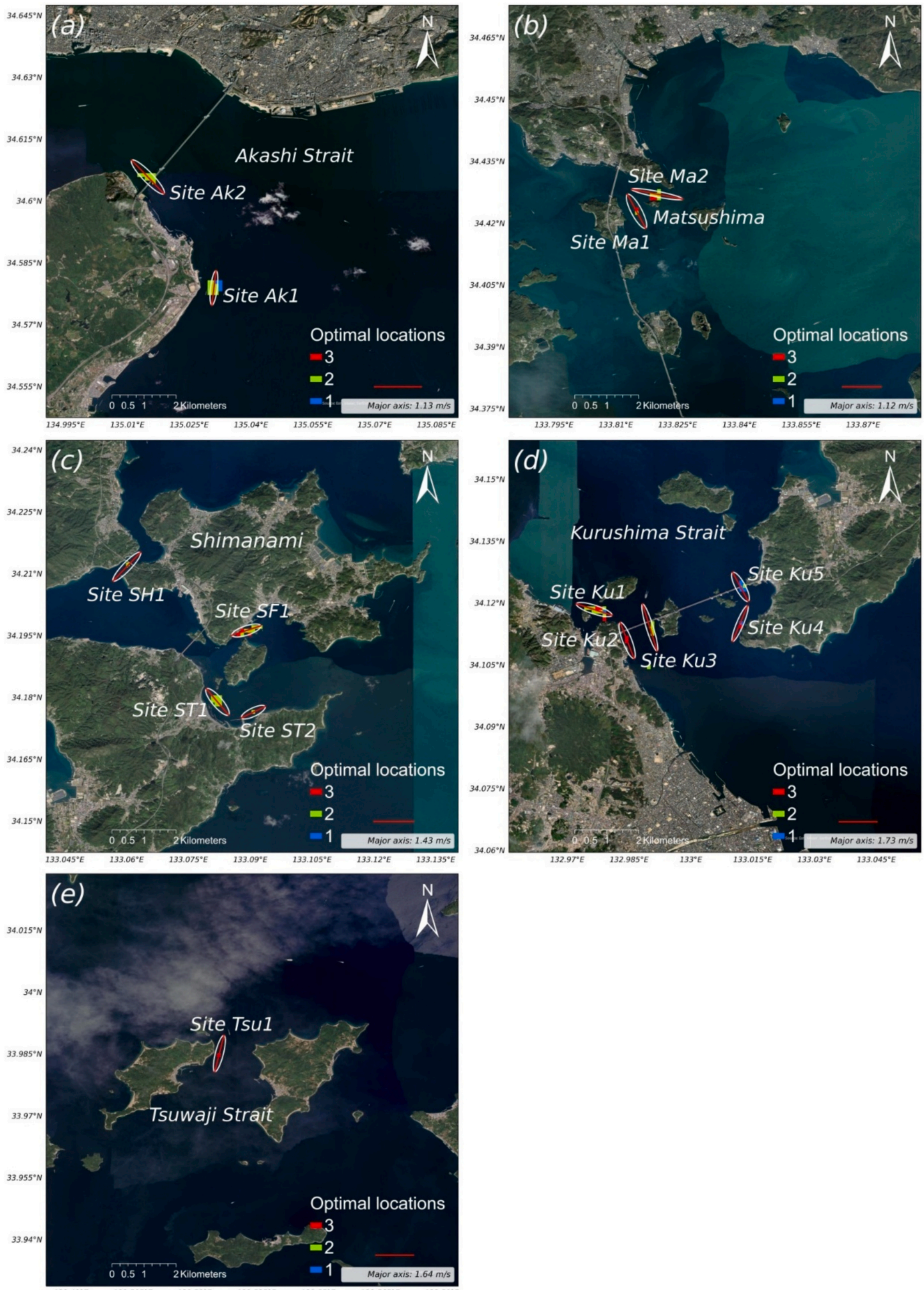

Fig. 2. Proposed tidal farms in the Seto Inland Sea along with the elliptical orientation of the M2 tide at each site: (a) Akashi farm (Sites Ak1 and Ak2), (b) Matsushima farm (Sites Ma1 and Ma2), (c) Shimanami farm (Hanaguri Site SH1, Funaori Site SF1, and Tsuwaji Sites ST1 and ST2), (d) Kurushima sites (Sites Ku1, Ku2, Ku3, Ku4, and Ku5), and (e) Tsuwaji (Site Tsu1). The values in the legend indicate the ranking of the optimal site with 3 is the best.

Table 2

Specification of tidal sites in the Seto Inland Sea starting with two sites on the Akashi tidal farm (Ak1, Ak2), three sites on the Matsushima-Obatake tidal farm (Ma1, Ma2) and (Ob1) [44], four sites on the Shimanami tidal farm (Hanaguri Strait (SH1), the Funaori Strait (SF1), Taizaki Island (ST1, ST2), and six sites on the Kurushima-Tsuwaji tidal farm (Ku1 ∼ Ku5), and (Tsu1). The cell resolution of the tidal sites is 100 × 100 m.

Tidal site	Site area ($10^4 \times m^2$)	Average depth (m)	Highest current velocity (m/s)	Turbine diameter D (m)	Turbine hub-height (m)	Rated velocity V_r (m/s)	Number of turbines	Coefficient of availability($\overline{C_{av}}$)
Ak1	15	29	2.5	18	−15	2.3	15	0.35
Ak2	9	35	2.2	20	−15	2	9	0.39
Ma1	2	26	2.16	16	−13	2	2	0.4
Ma2	7	29	2.43	18	−15	2.3	7	0.6
Ob1	37	22.5	3.5	13	−10	3	9	0.78
SH1	1	31	2.62	20	−15	2.5	1	0.55
SF1	10	34	2.6	20	−18	2.5	10	0.32
ST1	8	29	2.62	18	−15	2.5	8	0.37
ST2	1	32	2.18	20	−15	2	1	0.3
Ku1	12	36.7	3	20	−18	2.8	12	0.655
Ku2	2	21.5	3.22	12	−11	3	4	0.6
Ku3	4	64.7	3.56	20	−35	3	4	0.7
Ku4	2	32.7	3.6	20	−16	3	2	0.58
Ku5	5	52	2.84	20	−25	2.5	5	0.565
Tsu1	1	26.7	2.6	16	−13	2.4	1	0.613

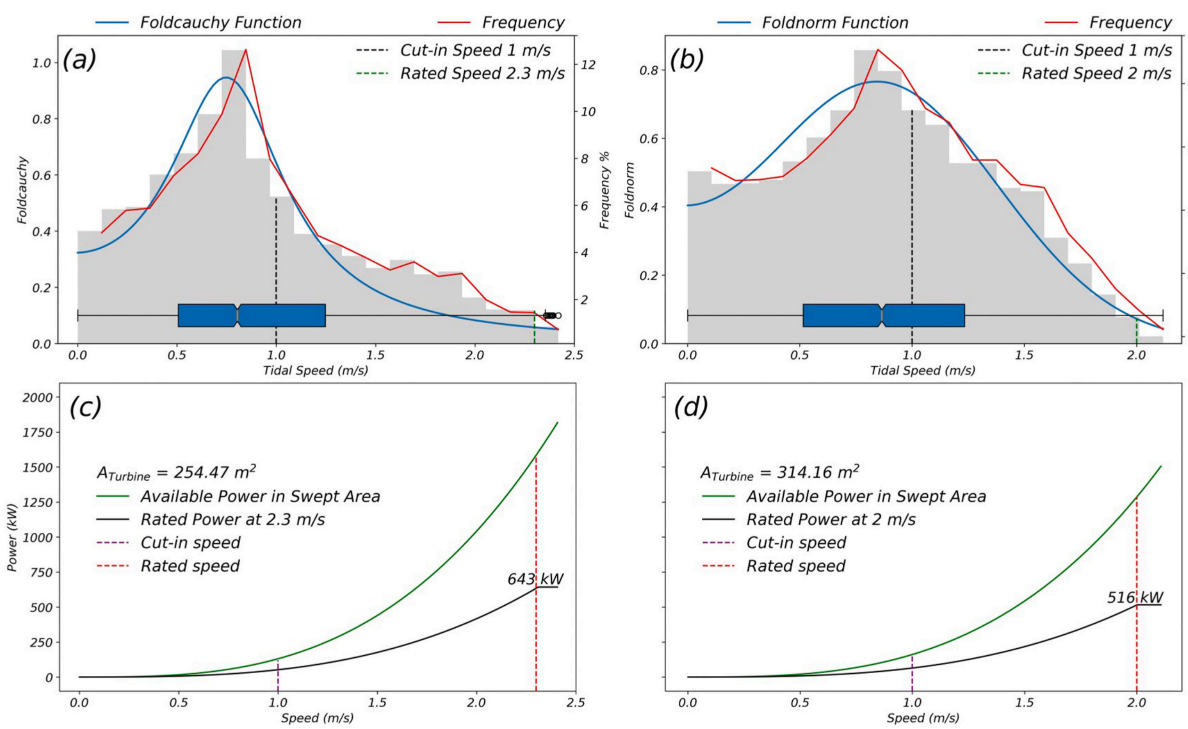

Fig. 3. Occurrence likelihood of the dominant velocity at Akashi Farm, the best fitted curve for the velocity distribution (Foldcauchy and Foldnorm) and the boxplot for the tidal velocity range and distribution along with the median velocity at the notch: (a) site Ak1, (b) site Ak2, (c) power calculation at site Ak1, (d) power calculation at site Ak2.

Table 3

Levelised cost of energy (LCOE) for four proposed tidal farms in the Seto Inland Sea under three scenarios (Japanese market assumption (JM), MeyGen prices (MG), and UK market assumption (UKM)) and two discount rates ($r = 10\%$ and $r = 5\%$) along with the turbine count, the power per farm (P_f) and the annual energy production (AEP).

Tidal farm	JM ¥/MWh	MG ¥/MWh	UKM ¥/MWh	JM ¥/MWh	MG ¥/MWh	UKM ¥/MWh	Turbine count	P_f (MW)	AEP (MWh/year)
	Discount rate (r) = 10%			Discount rate (r) = 5%					
Akashi	84,111	173,413	92,176	31,175	61,262	34,160	24	14.3	45,440
Matsushima & Obatake	44,553	91,855	44,320	16,513	32,450	16,440	18	12.16	73,000
Shimanami	87,117	179,609	63,449	32,288	63,451	23,526	20	18.24	56,000
Kurushima & Tsuwaji	48,095	99,159	24,093	17,826	35,030	8925	28	36	200,200
Average	65,969	136,000	56,000	24,450	48,048	20,763			
$LCOE_{ave}$		85,990			31,088				

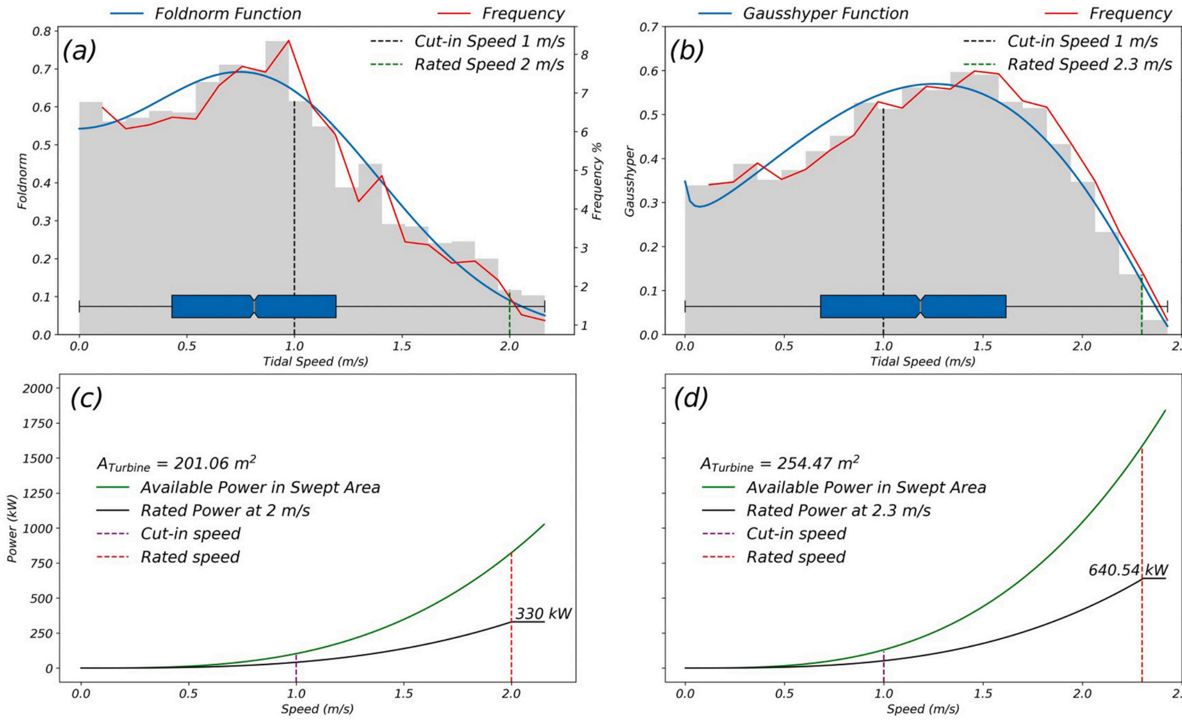

Fig. 4. Occurrence likelihood of the dominant velocity at Matsushima Farm, the best fitted curve for the velocity distribution (Foldnorm and Gausshyper) and the boxplot for the tidal velocity range and distribution along with the median velocity at the notch: (a) site Ma1, (b) site Ma2, (c) power calculation at site Ma1, (d) power calculation at site Ma2.

tidal sites are close in distance, and the relatively large installation volume in the SF1 (10 turbines) and Taizaki Island (ST1 and ST2) (9 turbines) balances the economy of the farm. Fig. 5 presents the likelihood of occurrence and the power calculation for the four sites. The power per turbine differed between the SH1 and SF1 even though the turbine specifications were the same. The reason is that the power was calculated on the basis of the velocity in each bin of the histogram.

For each site, the 56-day dominant current velocity at the hub height of the turbine was divided into 200 bins to provide an identical base for all calculations. The bin count was chosen to ensure that the upper limit of the final bin closely aligned with a whole number. Therefore, the power calculation was slightly different depending on the velocities stored in each bin. The power output was higher than the rated power for the SAE turbine (for a 2.5 m/s current velocity, the rated power was 1 MW; see Table 1). In reality, turbines might surpass the specification design or remain within it. The active tidal sites in MeyGen and Goto reported that power production was greater than expected [29,76].

The power per site for the SH1 was $P_{fSH1} = 1015.44 \times 1 = 1\,MW$, that for the SF1 was $P_{fSF1} = 1012.3 \times 10 = 10.12\,MW$, that for ST1 was $P_{fST1} = 822 \times 8 = 6.6\,MW$, and that for ST2 was $P_{fST2} = 520 \times 1 = 0.52\,MW$. Thus, the total power per farm was $P_f = 18.24\,MW$. For SH1, $AEP_{SH1} = 4.82$ GWh/year; for SF1, $AEP_{SF1} = 28.4$ GWh/year; for ST1 and ST2, $AEP_{ST1} = 21.4$ GWh/year; $AEP_{ST2} = 1.4$ GWh/year. Thus, the total $AEP = 56\,GWh/year$. The power per farm was greater than that of the Matsushima and Obatake tidal farms and greater than that of the Akashi tidal farm because of the larger number of 20 m diameter turbines. This increase negatively affected LCOE for Japanese market prices and for MeyGen prices (Table 3). Despite the greater diameter, the Shimanami tidal farm produced less AEP than the Matsushima and Obatake tidal farms did. The highest LCOE was 179,609 ¥/MWh for $r =$ 10% with the MeyGen Prices, and it dropped to 63,451 ¥/MWh for $r =$ 5%. On the other hand, the UK market price provided improved results because of the large turbine scale and sparse number. The LCOE was 63,449 ¥/MWh for $r =$ 10%, and it decreased to 23,526 ¥/MWh for $r =$ 5%.

3.5. *Kurushima strait and tsuwaji strait*

The Kurushima Strait is in the southern part of the Shimanami Islands between Oshima Island and mainland Shikoku Island. The Kurushima Strait is the largest among all straits within the archipelago and is approximately 1 km wide and 4 km long [77]. The Kurushima Strait is well known for its energetic tidal current, with velocities exceeding 3.5 m/s [78]. For shipping movements, the Kurushima Strait is the major connection between Hiuchi Nada and Aki Nada. Six optimal sites were identified in the Kurushima Strait. Tidal power calculations were conducted at five sites only because one site has a low frequency of high tidal velocity (Fig. 2d). The Tsuwaji Strait is in Ehime Prefecture between Tsuwaji and the Nuwa Islands. It is one of the straits that connects Aki Nada with Iyo Nada in the southern part of the SIS. One site was identified as a potential candidate for TPGs near the northern tip of Tsuwaji Island (Fig. 2e). The specifications for all tidal sites are displayed in Table 2. The major angles for M2 in the Kurushima Strait were 162.21°, 111.16°, 107.2°, 67.17°, and 118.55° for sites Ku1, Ku2, Ku3, Ku4, and Ku5, respectively. For the Tsuwaji site (Tsu1), the major angle for M2 was 75.73°. Twenty-seven turbines with a diameter of mostly 20 m could be installed in the Kurushima Strait alone, and one turbine could be installed in the Tsuwaji Strait. The occurrence likelihood and the power calculation are shown in **Figs. 6 and 7**. The power per farm was $P_f = 36\,MW$, with $32.5\,MW$ only from the Kurushima Strait. The total $AEP = 200.2\,GWh/year$. Power production was the highest among all farms in the SIS, leading to a competitive LOCE of 8925 ¥/MWh for $r = 5\%$ with UK market prices. The Japanese market price was also low, with LCOE equal to 17,826 ¥/MWh for $r = 5\%$ and 48,095 ¥/MWh for $r = 10\%$. The highest LCOE was in the MeyGen price scenario, with 99,159 ¥/MWh for $r = 10\%$ and 35,030 ¥/MWh for $r = 5\%$.

3.6. *Integrated annual energy production and tidal phasing effect*

The synthesis of AEP from all tidal farms was approximately 374,640,000 kWh/year. Using Eqs. (4) and (5), the number of

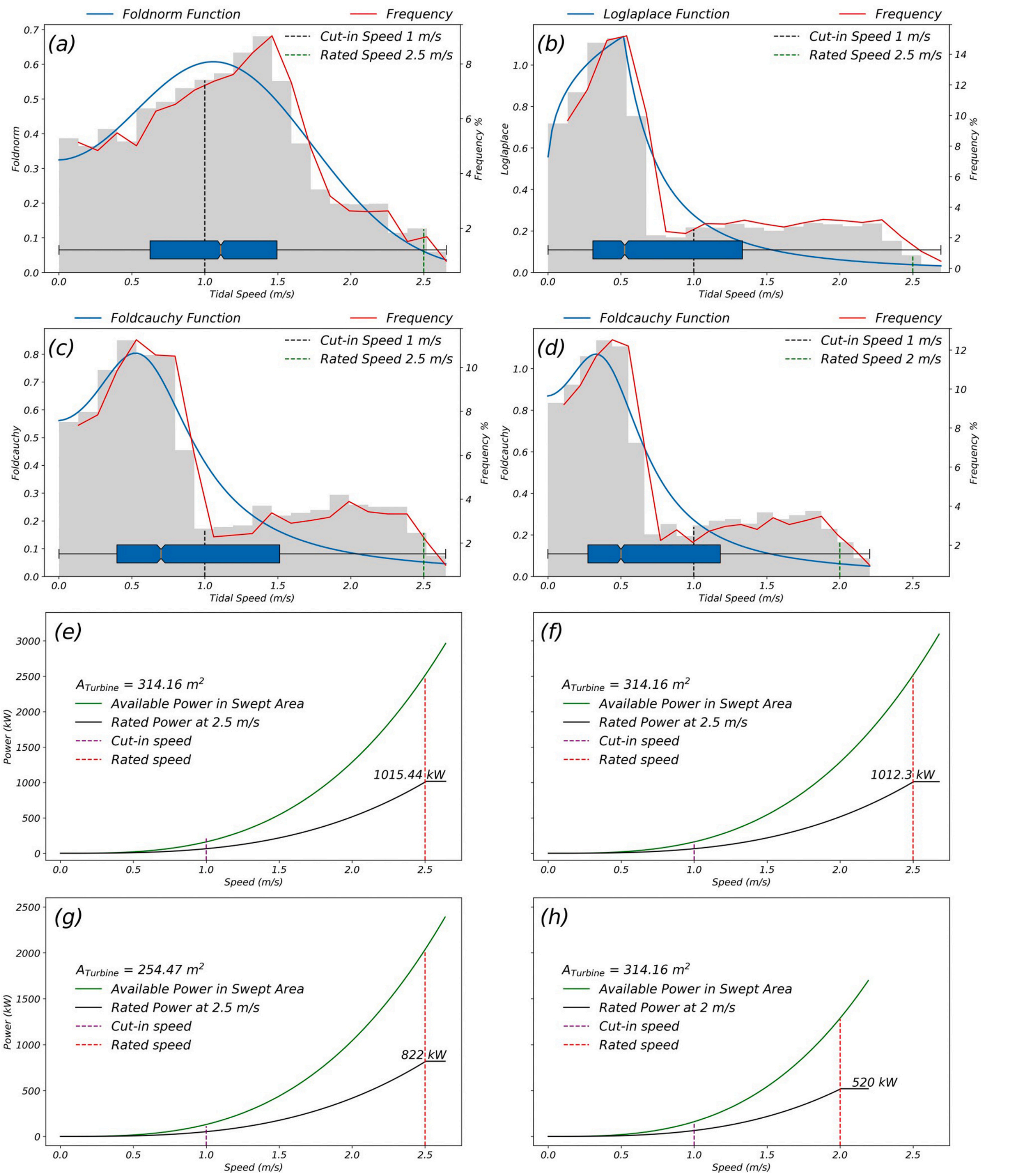

Fig. 5. Occurrence likelihood of the dominant velocity at Shimanami Farm, the best fitted curve for the velocity distribution (Foldnorm, Loglaplase, and Foldcauchy) and the boxplot for the tidal velocity range and distribution along with the median velocity at the notch, (a) Hanaguri Strait (site SH1), (b) Funaori Strait (site SF1), (c) Taizaki (site ST1), (d) Taizaki (site ST2), (e) power calculation in the Hanaguri Strait (site SH1), (f) power calculation in the Funaori Strait (site SF1), (g) power calculation in Taizaki (site ST1), (h) power calculation in Taizaki (site ST2).

households that dispensed electricity was approximately $N = 89,735$, and the CO_2 reduction was approximately $R_c = 166,000$ $ton\ CO_2/year$.

The SIS is connected to the Pacific Ocean through the Bungo Channel and Kii Channel and to the Japan Sea through the Kanmon Strait (Fig. 1). The water circulation in the SIS is contributed mainly by the Bungo and Kii channels, with a minor effect from the Kanmon Strait [67]. The tidal phase is almost coincident at all optimal locations (Fig. 8). This coincidence results in concurrent power production at all sites. Some tidal sites have flood tide dominance, such as SF1, where the velocity during the ebb tide is less than 1 m/s; some sites have ebb tide dominance, such as Ku4; and other sites have bidirectional tidal velocities, such as Ma2. Similar to tidal lagoons [79], the power output is consistent, which

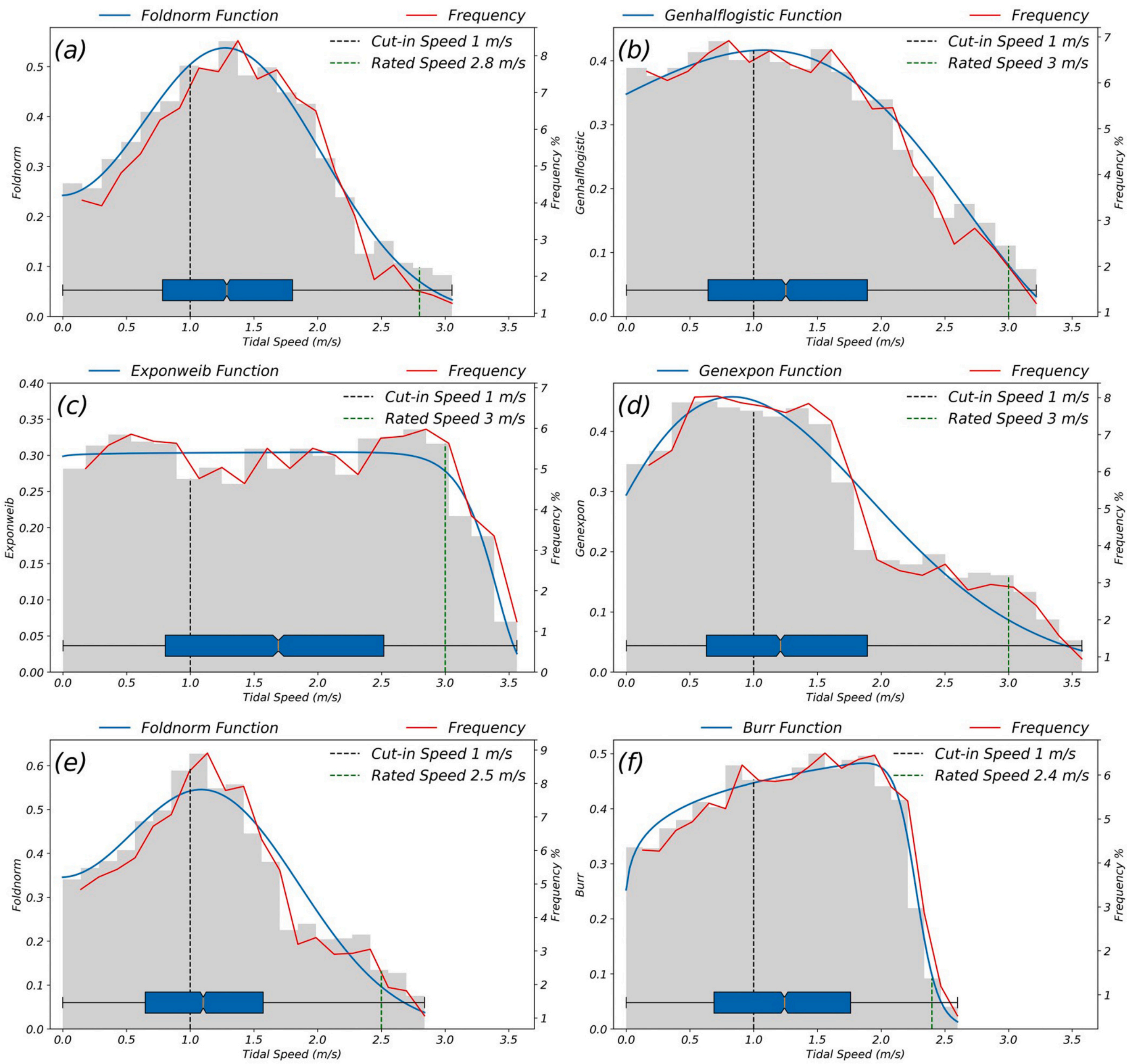

Fig. 6. Occurrence likelihood of the dominant velocity for the Kurushima and tsuwaji tidal farm, the best fitted curve for the velocity distribution (Foldnorm, Genhalflogistic, Exponweib, Genexpon, and Burr) and the boxplot for the tidal velocity range and distribution along with the median velocity at the notch, (a) Kurushima site Ku1, (b) Kurushima site Ku2, (c) Kurushima site Ku3, (d) Kurushima site Ku4, (e) Kurushima site Ku5, (f) Tsuwaji Strait (site Tsu1).

facilitates operation and demand control. Thus, uninterrupted power output is expected, especially if the cut-in velocity per turbine is reduced to 0.5 m/s. For TPGs, studies have shown that more than 90 % of the extracted tidal power can be exported to the grid, which limits the need for backup battery systems [80]. This power output improves the integration and management within the electricity grid, contributing to the overall renewable energy mix.

4. Discussion

4.1. Tidal power competitiveness

The capital cost of the TPG decreases with increasing installed capacity and learning rate. For example, increasing the cumulative capacity from 10 MW to 1 GW reduces the capital cost by approximately 3 % [39]. The learning rate is the reduction percentile in costs per doubling of installed capacity. For example, the learning rate is 10 % if the cost of power decreases by 10 % from the first MWh to the second MWh [30]. The tidal stream velocity also plays a critical role in determining the LCOE. A reduction in tidal velocity of 20 % can double the LCOE, underscoring the sensitivity of the TPG to site-specific conditions [35]. The design and deployment also contribute to cost reductions. For example, the development of a customised barge for turbine installation reduces the number of expensive dynamic positioning vessels. These innovations are expected to lower the installation costs for larger-scale tidal arrays [19].

Rodrigues et al. [81] reported an LCOE of 428 €/MWh for a small-scale turbine (35 kW) in Ria Formosa, Portugal. For a larger scale turbine (1200 kW), the estimated LCOE was 165 €/MWh [34]. Lamy et al. [82] estimated that the LCOE of the TPG for 2050 will range between 74 $/MWh and 330 $/MWh. A 10 MW tidal array in Tacoma Narrows in the USA is expected to have an LCOE of 400 $/MWh [83]. Bricker et al. [51]

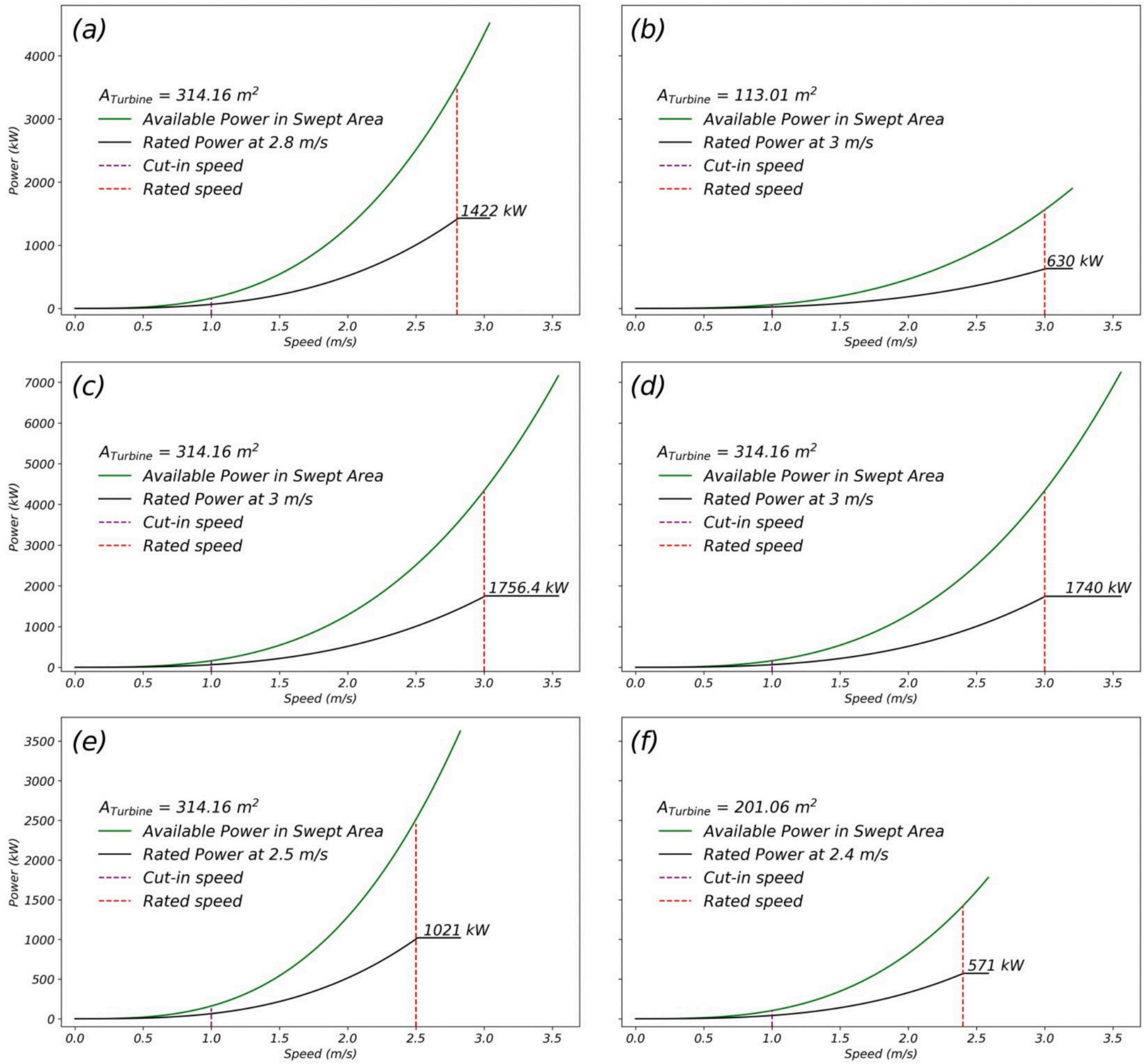

Fig. 7. Power calculations at the Kurushima and Tsuwaji tidal farm: (a) Kurushima site Ku1, (b) Kurushima site Ku2, (c) Kurushima site Ku3, (d) Kurushima site Ku4, (e) Kurushima site Ku5, and (f) Tsuwaji Strait (site Tsu1).

evaluated tidal energy farms in western Japan and reported that the LCOE could fall below 20,000 ¥/MWh, assuming farms with 1.2 MW turbines. Tidal farms with smaller turbines (38 kW) presented LCOE values below 16,000 ¥/MWh. The turbine price is lower for small-diameter turbines, but the installation and maintenance costs are not [19]. Therefore, it is more efficient to have larger turbines with higher rated power. Furthermore, the selection of a turbine must be based on site properties such as depth and tidal current velocity [84].

In this study, the average LCOE per discount rate (10 % and 5 %) for each scenario was calculated. The LCOE was then averaged for the 10 % discount rate and for the 5 % discount rate ($LCOE_{ave}$) (see Table 3). The $LCOE_{ave}$ for a 10 % discount rate was 85,990 ¥/MWh, and the $LCOE_{ave}$ for a 5 % discount rate was 31,088 ¥/MWh. At its current stage, TPG remains more expensive than wind and solar energy. However, with progressive technological advancements and industry maturation, these costs are anticipated to decline over time. Renewable energy in Japan relies on solar and onshore wind, with offshore wind expected to gain prominence in the coming years. According to the Ministry of Economy, Trade, and Industry (METI), the LCOE for solar power is 12,900 ¥/MWh, that for onshore wind is 19,800 ¥/MWh, and that for offshore wind is 30,000 ¥/MWh [85]. In comparison, the target LCOE for TPG in Japan at early consideration was higher at 36,000 ¥/MWh [46]. This study demonstrated that competitive LCOE is attainable and is affected mainly by AEP and supportive policies to lower risk and encourage large-scale investment.

4.2. *Prospects of tidal power in Japan*

The main barrier for TPGs in Japan could be the high cost. Other barriers might be market penetration and social impact, which are under addressed in the case of Japan. Effective strategies must be implemented to lower the cost and encourage the development of TPGs. At the MeyGen tidal site, a government subsides of approximately 20 % of the CAPEX was provided for the development of phase A1. It is more

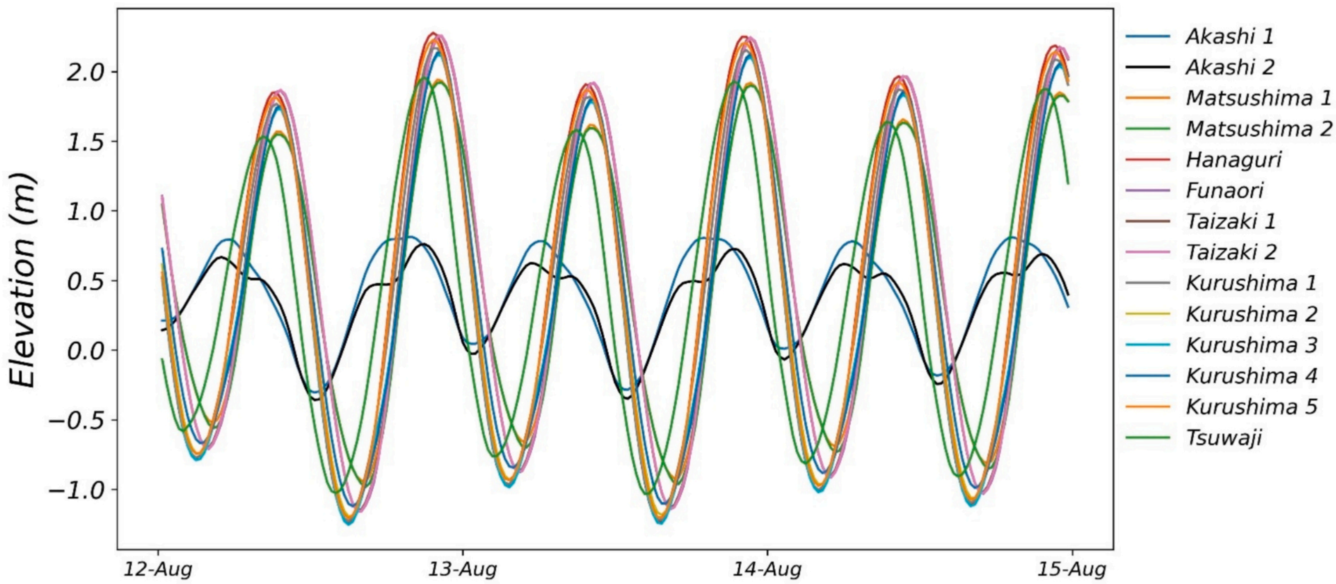

Fig. 8. Tidal elevation from all tidal sites in the Seto Inland Sea for three days.

efficient for Japanese developers to manufacture tidal turbines, which will lower the total cost of tidal farms and create opportunities for investment [86].

For TPGs, installation, maintenance, and operation have negligible environmental impacts across all device types [87]. In contrast, the environmental footprint of fossil fuel plants is primarily concentrated in the operational phase. Japan consists of numerous remote islands with small communities, especially in the SIS, and the TPG offers positive economic and social benefits [88]. Furthermore, the TPG eliminates the cost of cable connection with the mainland. These advantages, combined with cost-reduction strategies and site-specific optimisation, illustrate the significant potential of TPG as a sustainable and economically viable renewable energy source.

4.3. Sensitivity analysis for LCOE

The LCOE is affected by many factors, and it is difficult to predict an exact number, especially for the TPG. The results of the above analysis suggest that the LCOE is influenced mainly by the AEP and discount rate (r). In the case of the SIS, farm four (Kurushima and Tsuwaji) had the optimal scoring LCOE of 8925 ¥/MWh and AEP of 200.2 GWh/year for r equal to 5 % under the third scenario (the UK market assumption) (Table 3). Therefore, farm four, with the optimal LCOE, was used to discuss the sensitivity of several parameters. Fig. 9 presents the results of the sensitivity analysis. As expected, for r values ranging between 5 % and 15 %, the change in LCOE was the most extreme (Fig. 9 **a**). When r is equal to 15 %, the LCOE reaches 69,000 ¥/MWh, which is approximately eight times the optimal value. For AEP, the analysis encompassed a reduction percentile between 10 % and 50 % from the original AEP. The AEP is calculated using the output power from the farm, which is compromised by the tidal current available for power generation. At this time, there are no fully commissioned tidal farms in the world, and the information regarding the optimal positioning and distribution of the turbines inside the farm remains at the research level. The LCOE was less influenced by AEP than by r. For a 10 % reduction in AEP, the LCOE was approximately 9917 ¥/MWh. The LCOE increased to approximately

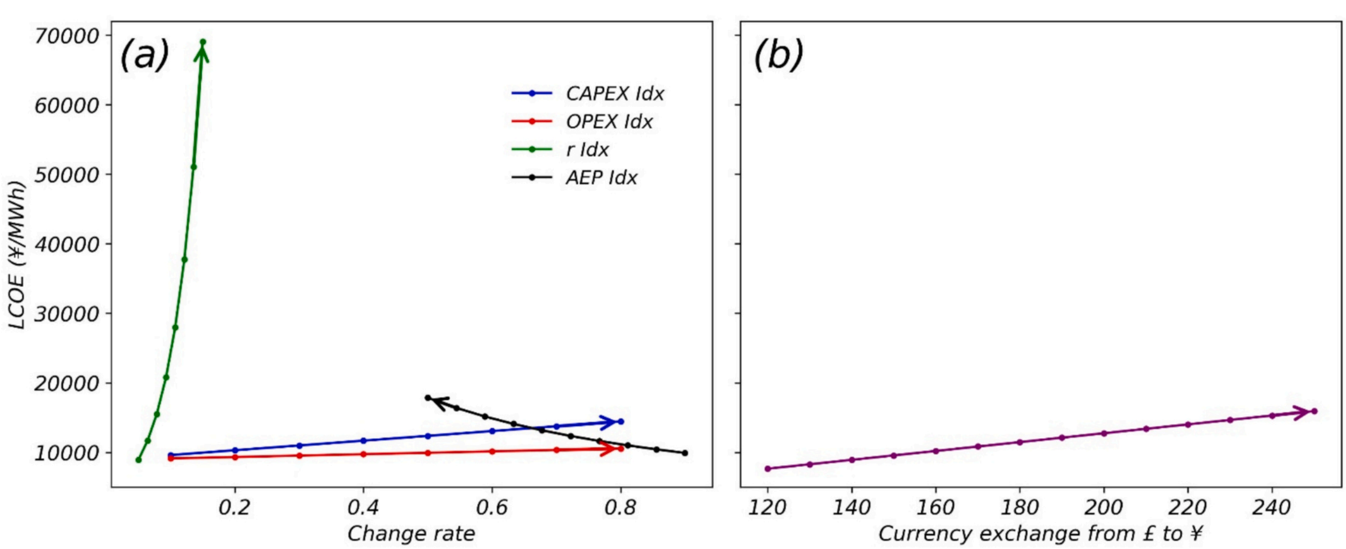

Fig. 9. (a) Sensitivity analysis of the levelised cost of energy (LCOE) with increasing capital expenditure (CAPEX), operation expenditure (OPEX), and discount rate (r) and decreasing annual energy production (AEP). (b) Sensitivity of the LCOE for the exchange rate between the GBP (£) and JPY (¥).

17,850 ¥/MWh for a 50 % reduction in AEP (Fig. 9.**a**). Fig. 9.**a** shows that the influence of increased CAPEX and OPEX had the smallest effect on the LCOE. For 80 % increases in CAPEX and OPEX, the LCOEs were 14,442 ¥/MWh and 10,549 ¥/MWh, respectively.

The exchange rate between the GBP and JPY causes uncertainty in the cost analysis due to sharp fluctuations over time. The choice of 1 GBP equal to 140 JPY is based on a relatively stable period before COVID-19. Therefore, an exchange rate between (1 GBP equal to 120 JPY) and (1 GBP equal to 250 JPY) was used to investigate the influence of the exchange rate on the LCOE. Fig. 9.**b** shows that even for the highest rate of 250, the LCOE was 15,938 ¥/MWh. This effect remains small compared with that of AEP and r.

5. Conclusion

The TPG presents a promising addition to the renewable energy portfolio, offering reliable and predictable energy generation that can complement variable sources such as solar and wind. This study provides a feasibility assessment of the potential of the TPG in the SIS in Japan. Four tidal farms were proposed. The Akashi Strait; Matsushima Island and Obatake Strait; Shimanami Islands; Kurushima Strait and Tsuwaji Strait. The integrated AEP from all farms was 374.64 GWh/year, which can supply approximately 89,735 households and results in an approximately 166,000 tons of CO_2 reduction per year.

The LCOE was used to conduct economic analysis for each tidal farm. Three scenarios were used for the CAPEX and OPEX assumptions, and two discount rates of 10 % and 5 % were used. The $LCOE_{ave}$ among the three scenarios for a 10 % discount rate was approximately 85,990 ¥/MWh, and the $LCOE_{ave}$ for a 5 % discount rate was 31,088 ¥/MWh. Despite the current higher cost for TPG, continued technological advancements, scaling of installed capacity, and innovations in installation and maintenance processes are expected to reduce the LCOE.

The 100 m resolution of the tidal model may introduce uncertainties in LCOE estimation by limiting the accuracy of flow dynamics at finer scales. Additionally, the wake effect on power production was not considered in this study, which led to an underestimation of energy losses and impact cost projections. Currency exchange rates also influence LCOE calculations, as fluctuations affect capital and operational expenditures, particularly for imported components. Furthermore, the discount rate assumption significantly impacts LCOE, with lower rates improving economic feasibility.

In Japan, the deployment of TPGs faces unique challenges, including high initial costs and limited specialised infrastructure. Addressing these barriers requires governmental support to modernise infrastructure, streamline permitting processes, and incentivise private investment. As Japan continues to transition to a low-carbon energy system, integrating TPG alongside solar, wind, and other renewables could play a crucial role in achieving energy security and environmental sustainability. While there is still much to be done to overcome the current economic and logistical challenges, the long-term potential of TPG to contribute to decarbonisation efforts and enhance grid stability makes it a valuable area for continued research, development, and policy support.

CRediT authorship contribution statement

Morhaf Aljber: Writing – original draft, Visualization, Validation, Software, Resources, Methodology, Investigation, Formal analysis, Data curation, Conceptualization. **Han Soo Lee:** Writing – review & editing, Writing – original draft, Supervision, Resources, Project administration, Investigation, Funding acquisition, Formal analysis, Data curation, Conceptualization. **Jae-Soon Jeong:** Investigation, Formal analysis.

Declaration of competing interest

The authors declare that they have no known competing financial interests or personal relationships that could have appeared to influence the work reported in this paper.

Acknowledgement

The first author would like to thank the Hiroshima University SPRING Research fellowship for supporting this study. The tidal current used is based on the Japanese Coastal Ocean Monitoring and Forecasting System (MRI. COM-JPN) developed by the Meteorological Research Institute of the Japan Meteorological Agency, Japan. This study is supported by the JSPS Grant-in-Aid for Scientific Research (B) (Grant No. 24 K00991).

Data availability

Data will be made available on request.

References

[1] NRDC. The Paris agreement on climate Change. 2017. https://www.nrdc.org/sites/default/files/paris-agreement-climate-change-2017-ib.pdf. accessed January 11, 2025.
[2] Esteban M, Portugal-Pereira J, Mclellan BC, Bricker J, Farzaneh H, Djalilova N, et al. 100% renewable energy system in Japan: smoothening and ancillary services. Appl Energy 2018;224:698–707. https://doi.org/10.1016/j.apenergy.2018.04.067.
[3] Icaza D, Vallejo-Ramirez D, Guerrero Granda C, Marín E. Challenges, Roadmaps and smart energy transition towards 100% renewable energy markets in american Islands: a review. Energies (Basel) 2024:17. https://doi.org/10.3390/en17051059.
[4] Al-Shetwi AQ, Abidin IZ, Mahafzah KA, Hannan MA. Feasibility of future transition to 100% renewable energy: recent progress, policies, challenges, and perspectives. J Clean Prod 2024:478. https://doi.org/10.1016/j.jclepro.2024.143942.
[5] Buzzi F, Bischi A, Gabbrielli R, Desideri U. Hourly electrical load estimates in a 100% renewable scenario in Italy. Renew Energy 2025:239. https://doi.org/10.1016/j.renene.2024.122089.
[6] Ahmed F, Foley A, McLoone S, Best R, Lund H, Al Kez D. Sectoral coupling pathway towards a 100% renewable energy system for Northern Ireland. Renew Sust Energ Rev 2025:210. https://doi.org/10.1016/j.rser.2024.114939.
[7] Zhong J, Bollen M, Rönnberg S. Towards a 100% renewable energy electricity generation system in Sweden. Renew Energy 2021;171:812–24. https://doi.org/10.1016/j.renene.2021.02.153.
[8] Hansen K, Mathiesen BV, Skov IR. Full energy system transition towards 100% renewable energy in Germany in 2050. Renew Sust Energ Rev 2019;102:1–13. https://doi.org/10.1016/j.rser.2018.11.038.
[9] García-Olivares A, Solé J, Osychenko O. Transportation in a 100% renewable energy system. Energy Convers Manag 2018;158:266–85. https://doi.org/10.1016/j.enconman.2017.12.053.
[10] Climate Council. 11 countries leading the charge on renewable energy. https://www.climatecouncil.org.au/11-countries-leading-the-charge-on-renewable-energy/?utm_source. [Accessed 11 January 2025].
[11] Spector Julian. (2023 November 17). Portugal just ran on 100% renewables for six days in a row. Canary Media. https://www.canarymedia.com/articles/clean-energy/portugal-just-ran-on-100-renewables-for-six-days-in-a-row?utm_source [accessed January 11, 2025].
[12] Wei Y, Khojasteh D, Windt C, Huang L. An interdisciplinary literature review of floating solar power plants. Renew Sust Energ Rev 2025:209. https://doi.org/10.1016/j.rser.2024.115094.
[13] Le Lim X, Lam WH. Public acceptance of marine renewable energy in Malaysia. Energy Policy 2014;65:16–26. https://doi.org/10.1016/j.enpol.2013.09.053.
[14] Caballero MD, Gunda T, McDonald YJ. Energy justice & coastal communities: the case for meaningful marine renewable energy development. Renew Sust Energ Rev 2023:184. https://doi.org/10.1016/j.rser.2023.113491.
[15] Borràs Mora E, Spelling J, van der Weijde AH. Global sensitivity analysis for offshore wind cost modelling. Wind Energy 2021;24:974–90. https://doi.org/10.1002/we.2612.
[16] Ma Y, Zhao R, Zhao W, Tai B, Dong G. Dynamic analysis to reduce the cost for fixed offshore wind energy turbines. Appl Energy 2025:378. https://doi.org/10.1016/j.apenergy.2024.124804.
[17] Kausche M, Adam F, Dahlhaus F, Großmann J. Floating offshore wind - economic and ecological challenges of a TLP solution. Renew Energy 2018;126:270–80. https://doi.org/10.1016/j.renene.2018.03.058.
[18] Johnston B, Foley A, Doran J, Littler T. Levelised cost of energy, a challenge for offshore wind. Renew Energy 2020;160:876–85. https://doi.org/10.1016/j.renene.2020.06.030.
[19] Goss Z, Coles D, Piggott M. Economic analysis of tidal stream turbine arrays: A review. 2021.
[20] Pennock S, Noble DR, Vardanyan Y, Delahaye T, Jeffrey H. A modelling framework to quantify the power system benefits from ocean energy deployments. 2023. https://doi.org/10.7488/ds/7469.
[21] Coles D, Angeloudis A, Greaves D, Hastie G, Lewis M, MacKie L, et al. A review of the UK and British Channel Islands practical tidal stream energy resource. Proc

Royal Soc A: Math, Phys Eng Sci 2021;477. https://doi.org/10.1098/rspa.2021.0469.
[22] Lewis M, McNaughton J, Márquez-Dominguez C, Todeschini G, Togneri M, Masters I, et al. Power variability of tidal-stream energy and implications for electricity supply. Energy 2019;183:1061–74. https://doi.org/10.1016/j.energy.2019.06.181.
[23] Garcia-Novo P, Coles D, Kyozuka Y, Yamada R, Moriguchi H, Sakaguchi D. Optimization of a tidal–wind–solar system to enhance supply–demand balancing and security: a case study of the goto Islands, Japan. Sustainability 2023;15:9147. https://doi.org/10.3390/su15129147.
[24] Coles D, Angeloudis A, Goss Z, Miles J, Tidal stream vs.. Wind energy: the value of cyclic power when combined with short-term storage in hybrid systems. Energies (Basel) 2021:14. https://doi.org/10.3390/en14041106.
[25] Khojasteh D, Shamsipour A, Huang L, Tavakoli S, Haghani M, Flocard F, et al. A large-scale review of wave and tidal energy research over the last 20 years. Ocean Eng 2023:282. https://doi.org/10.1016/j.oceaneng.2023.114995.
[26] Li G, Zhu W. Tidal current energy harvesting technologies: a review of current status and life cycle assessment. Renew Sust Energ Rev 2023:179. https://doi.org/10.1016/j.rser.2023.113269.
[27] Gu Y, Zou T, Liu H, Lin Y, Ren H, Li Q. Status and challenges of marine current turbines: a global review. J Mar Sci Eng 2024:12. https://doi.org/10.3390/jmse12060884.
[28] Bae YH, Kim KO, Choi BH. Lake Sihwa tidal power plant project. Ocean Eng 2010; 37:454–63. https://doi.org/10.1016/j.oceaneng.2010.01.015.
[29] Cohen Claire, Baker Tim. Lessons learnt from MeyGen phase 1A final summary Report. https://webassets.bv.com/2020-06/MeyGen%20Lessons%20Learnt%20Full%20Report_0.pdf. [Accessed 13 January 2025].
[30] Walker S, Thies PR. A review of component and system reliability in tidal turbine deployments. Renew Sust Energ Rev 2021:151. https://doi.org/10.1016/j.rser.2021.111495.
[31] Kyuden Mirai Ltd. First demonstration test of commercial-scale large-scale tidal current power generation in Japan. 2022.
[32] Yang Z, Ren Z, Li Z, Xu Y, Li H, Li W, et al. A comprehensive analysis method for levelized cost of energy in tidal current power generation farms. Renew Energy 2022;182:982–91. https://doi.org/10.1016/j.renene.2021.11.026.
[33] Santhakumar S, Meerman H, Faaij A. Future costs of key emerging offshore renewable energy technologies. Renew. Energy 2024:222. https://doi.org/10.1016/j.renene.2023.119875.
[34] López A, Morán JL, Núñez LR, Somolinos JA. Study of a cost model of tidal energy farms in early design phases with parametrization and numerical values. Application to a second-generation device. Renew Sust Energ Rev 2020:117. https://doi.org/10.1016/j.rser.2019.109497.
[35] Bianchi M, Arnal AJ, Astorkiza-Andres M, Clavell-Diaz J, Marques A, Isasa-Sarralde M. Life cycle and economic assessment of tidal energy farms in early design phases: application to a second-generation tidal device. Heliyon 2024:10. https://doi.org/10.1016/j.heliyon.2024.e32515.
[36] Blaxland D, Johnson F, Macfarlane D, Robinson NJ. Cost reductions through smart transportation and installation engineering-experience of the MeyGen Tidal Array. https://apollo.engineer/wp-content/uploads/2022/07/CORE-2019-Paper-Meygen-project-TI-learning-final-rev0.pdf. [Accessed 12 January 2025].
[37] Murray J. Orbital marine power orbital O2.2 tidal turbine emec berth 6, fall of warness, eday, orkney project information Document. 2021. https://marine.gov.scot/sites/default/files/project_information_document.pdf. [Accessed 13 January 2025].
[38] Arup O. Department of Energy and Climate Change Review of renewable electricity generation cost and technical assumptions study Report job number job number review of renewable electricity generation cost and technical assumptions study Report Report ref | final |. www.arup.com. [Accessed 12 January 2025].
[39] Smart G, Noonan M. Tidal stream and wave energy cost reduction and industrial benefit summary analysis. 2018. https://www.marineenergywales.co.uk/wp-content/uploads/2018/05/ORE-Catapult-Tidal-Stream-and-Wave-Energy-Cost-Reduction-and-Ind-Benefit-FINAL-v03.02.pdf [accessed January 9, 2025].
[40] The Electric Power Industry in Japan. https://www.jepic.or.jp/en/data/pdf/epijJepic2023.pdf. [Accessed 13 January 2025].
[41] Kyuden Mirai Ltd. Commencement of installation of Japan's first commercial-scale large-scale Tidal current generator (completed modification of tidal current generator and installed off the coast of Goto City, Nagasaki Prefecture). 2025. https://www.q-mirai.co.jp/files/optionallink/00000596_file.pdf?1738897115 [accessed February 17, 2025].
[42] Garcia Novo P, Kyozuka Y. Tidal stream energy as a potential continuous power producer: a case study for West Japan. Energy Convers Manag 2021:245. https://doi.org/10.1016/j.enconman.2021.114533.
[43] Jeong J-S, Lee HS. Unstructured Grid-Based River–Coastal Ocean Circulation Modeling towards a Digital Twin of the Seto Inland Sea. Appl Sci 2023;13:8143. https://doi.org/10.3390/app13148143.
[44] Aljber M, Jeong J-S, Cabrera JS, Calvo MAS, Chisale SW, Williams Z, et al. Optimal site selection and potential power assessment for tidal power generation in the Seto Inland Sea, Japan, based on high-resolution ocean modelling and multicriteria analysis. Appl Energy 2024;372:123843. https://doi.org/10.1016/j.apenergy.2024.123843.
[45] Aljber M, Sakanoue G, Jeong J-S, Cabrera JS, Lee HS. Assessment of potential Tidal power sites in the Seto Inland Sea, Japan using multi-criteria evaluation. In: Caetano NS, Felgueiras MC, editors. The 9th international conference on energy and environment research. Cham: Springer Nature Switzerland; 2023. p. 281–9.
[46] MOE. Development and demonstration project of a 1 MW-class tidal current power generation system to expand the use of marine energy in Japan. 2015.
[47] Goss ZL, Coles DS, Kramer SC, Piggott MD. Efficient economic optimisation of large-scale tidal stream arrays. Appl Energy 2021:295. https://doi.org/10.1016/j.apenergy.2021.116975.
[48] Cornett A, Nistor I, Toupin M. Appraisal of IEC technical specification for Tidal energy resource assessment at Minas passage, Bay of Fundy, Canada. 2015.
[49] Cornett A, Baker S, Piche S, Nistor I, Toupin M. Appraisal of IEC standards for wave and Tidal energy resource assessment. 2014.
[50] Lee HS, Shimoyama T, Popinet S. Impacts of tides on tsunami propagation due to potential Nankai trough earthquakes in the Seto Inland Sea, Japan. J Geophys Res Oceans 2015;120:6865–83. https://doi.org/10.1002/2015JC010995.
[51] Bricker JD, Esteban M, Takagi H, Roeber V. Economic feasibility of tidal stream and wave power in post-Fukushima Japan. Renew Energy 2017;114:32–45. https://doi.org/10.1016/j.renene.2016.06.049.
[52] European Marine Energy Centre Ltd Assessment of Tidal energy resource. Tech Rep EMEC 2009. ISBN 978-0-580-65642-2. https://www.emec.org.uk/assessment-of-tidal-energy-resource/ accessed February 15, 2024.
[53] Marsh P, Penesis I, Nader JR, Cossu R. Multi-criteria evaluation of potential Australian tidal energy sites. Renew Energy 2021;175:453–69. https://doi.org/10.1016/j.renene.2021.04.093.
[54] Lande-Sudall D, Stallard T, Stansby P. Co-located offshore wind and tidal stream turbines: assessment of energy yield and loading. Renew Energy 2018;118:627–43. https://doi.org/10.1016/j.renene.2017.10.063.
[55] Lewis MJ, Neill SP, Hashemi MR, Reza M. Realistic wave conditions and their influence on quantifying the tidal stream energy resource. Appl Energy 2014;136:495–508. https://doi.org/10.1016/j.apenergy.2014.09.061.
[56] NEDO. Guidebook for Introducing Bottom-Fixed Offshore Wind Power. 2018. https://www.nedo.go.jp/content/100889993.pdf. accessed December 4, 2024.
[57] Barquero Carlos García, Saitou Tetsuo. Study on Best practices in Floating Offshore Wind Energy Technical Regulations in the EU and Member States. 2024. https://op.europa.eu/en/publication-detail/-/publication/e4a38ca6-aae9-11ef-acb1-01aa75ed71a1/language-en. accessed January 16, 2025.
[58] MOE. Demonstration Project of 2MW-class Tidal Current Power Generation System for Practical Use of Marine Renewable Energy. 2018. https://xn–env-gw2e922w.go.jp/content/900449568.pdf. accessed December 4, 2024.
[59] Tidal stream industry energiser. Cost reduction pathway of tidal stream energy in the UK and France Disclaimer. 2022. https://cms.ore.catapult.org.uk/wp-content/uploads/2022/10/Tidal-stream-cost-reduction-report-T3.4.1-v1.0-for-ICOE.pdf. accessed April 21, 2025.
[60] Nova Innovation. 19-HMAR-00499_Nova-Tidal-Array_Authorization_redacted. 2022. https://www.novatidalarray.ca/post/nova-receives-dfo-authorization [accessed February 20, 2025].
[61] Karsten Richard, Hay Alex, Jeans Tiger. Andrew Gerber, Dean Steinke, Greg Trowse. Reducing the cost of in-stream tidal energy generation through comprehensive hydrodynamic site assessment. https://natural-resources.canada.ca/funding-partnerships/reducing-cost-stream-tidal-energy-generation-through-comprehensive-hydrodynamic-site-assessment. [Accessed 21 April 2025].
[62] Fisheries and Oceans Canada. Task force on sustainable Tidal energy development in the bay of Fundy : Final report. Fisheries and Oceans Canada = Pêches et océans Canada. https://www.dfo-mpo.gc.ca/pnw-ppe/ffhpp-ppph/publications/fundy-tidal-final-report-baie-fundy-marees-rapport-final-eng.html; 2024.
[63] Chen H, Li Q, Benbouzid M, Han J, Aït-Ahmed N. Development and research status of tidal current power generation systems in China. J Mar Sci Eng 2021:9. https://doi.org/10.3390/jmse9111286.
[64] Coles D, Adcock T, Cornett A, Haas K, Jo CH, Liu H, et al. A review of global tidal stream energy resources. 2024. https://doi.org/10.31224/4078.
[65] Iyer AS, Couch SJ, Harrison GP, Wallace AR. Variability and phasing of tidal current energy around the United Kingdom. Renew Energy 2013;51:343–57. https://doi.org/10.1016/j.renene.2012.09.017.
[66] Kyuden Mirai Ltd. PRESS RELEASE. 2022.
[67] Jeong JS, Lee HS, Mori N. Abnormal surges and the effects of the Seto Inland Sea circulation in Hiroshima Bay, Japan. Front Mar Sci 2024:11. https://doi.org/10.3389/fmars.2024.1359288.
[68] MOE. Statistical Survey of CO2 Emissions from the Household Sector. 2022. https://www.env.go.jp/content/000084571.pdf. accessed December 19, 2024.
[69] Badouard T, Moreira De Oliveira D, Yearwood J, Rotterdam Torres P. Client: European Commission-DG Energy A4 Final Report-Cost of Energy (LCOE) Study on energy costs, taxes and the impact of government interventions on investments in the energy sector. 31 July 2020. p. 2020. https://energy.ec.europa.eu/system/files/2020-10/final_report_levelised_costs_0.pdf?utm_source. [Accessed 18 December 2024].
[70] Musial W, Spitsen P, Duffy P, Beiter P, Shields M, Mulas Hernando D, et al. Offshore wind market report. 2023. p. 2023. https://www.energy.gov/sites/default/files/2023-09/doe-offshore-wind-market-report-2023-edition.pdf?utm_source. [Accessed 19 January 2025].
[71] Neill Lee. 2016/ARP002-the Tidal turbine reef (TTR) feasibility study. https://arena.gov.au/assets/2017/02/tidal-turbine-reef-TTR-feasibility-study-report.pdf. [Accessed 19 January 2025].
[72] Stehly T, Duffy P, Mulas Hernando D. Cost Wind Energy Rev 2022:2023. https://www.nrel.gov/docs/fy24osti/88335.pdf?utm_source=chatgpt.com. [Accessed 18 December 2024].
[73] Goss ZL, Coles DS, Piggott MD. Identifying economically viable tidal sites within the Alderney race through optimization of levelized cost of energy: economic viability of the Alderney race. Philosophical Trans Royal Soc A: Math, Phys Eng Sci 2020:378. https://doi.org/10.1098/rsta.2019.0500.
[74] Coles DS, Blunden LS, Bahaj AS. The energy yield potential of a large tidal stream turbine array in the Alderney race: energy yield estimate for Alderney race.

Philosophical Trans Royal Soc A: Math, Phys Eng Sci 2020:378. https://doi.org/10.1098/rsta.2019.0502.
[75] Garcia-Novo P, Inubuse M, Matsuno T, Kyozuka Y, Archer P, Matsuo H, et al. Characterization of the wake generated downstream of a MW-scale tidal turbine in Naru Strait, Japan, based on vessel-mounted ADCP data. Energy 2024:299. https://doi.org/10.1016/j.energy.2024.131453.
[76] Kyuden Mirai Energy Ltd. Tidal power generation technology demonstration project of Goto Nagasaki. https://www.env.go.jp/content/000080123.pdf. [Accessed 15 December 2024].
[77] Adityawarman Y, Kaneko A, Taniguchi N, Mutsuda H, Gohda N. Reciprocal sound transmission measurement of the 5-day temperature variation in the Kurushima Strait. Acoust Sci Technol 2012;33:59–63. https://doi.org/10.1250/ast.33.59.
[78] Adityawarman Y, Kaneko A, Taniguchi N, Mutsuda H, Komai K, Guo X, et al. Tidal current measurement in the Kurushima Strait by the reciprocal sound transmission method. Acoust Sci Technol 2012;33:45–51. https://doi.org/10.1250/ast.33.45.
[79] Mackie L, Kramer SC, Piggott MD, Angeloudis A. Assessing impacts of tidal power lagoons of a consistent design. Ocean Eng 2021:240. https://doi.org/10.1016/j.oceaneng.2021.109879.
[80] Manchester S, Barzegar B, Swan L, Groulx D. Energy storage requirements for in-stream tidal generation on a limited capacity electricity grid. Energy 2013;61:283–90. https://doi.org/10.1016/j.energy.2013.08.036.
[81] Rodrigues N, Pintassilgo P, Calhau F, González-Gorbeña E, Pacheco A. Cost-benefit analysis of tidal energy production in a coastal lagoon: the case of ria Formosa – Portugal. Energy 2021:229. https://doi.org/10.1016/j.energy.2021.120812.
[82] Lamy JV, Azevedo IL. Do tidal stream energy projects offer more value than offshore wind farms? A case study in the United Kingdom. Energy Policy 2018;113:28–40. https://doi.org/10.1016/j.enpol.2017.10.030.
[83] Topper MBR, Olson SS, Roberts JD. On the benefits of negative hydrodynamic interactions in small tidal energy arrays. Appl Energy 2021:297. https://doi.org/10.1016/j.apenergy.2021.117091.
[84] Encarnacion JI, Johnstone C, Ordonez-Sanchez S. Design of a horizontal axis tidal turbine for less energetic current velocity profiles. J Mar Sci Eng 2019:7. https://doi.org/10.3390/jmse7070197.
[85] METI. Power Generation Cost Verification. 2024. https://www.enecho.meti.go.jp/committee/council/basic_policy_subcommittee/mitoshi/cost_wg/2024/data/05_05.pdf. accessed January 24, 2025.
[86] Mirai Kyuden. Power generation has started in the tidal power generation demonstration project off the coast of Singapore. https://www.q-mirai.co.jp/files/optionallink/00000458_file.pdf?1735172586. [Accessed 24 January 2025].
[87] Uihlein A. Life cycle assessment of ocean energy technologies. Int J Life Cycle Assess 2016;21:1425–37. https://doi.org/10.1007/s11367-016-1120-y.
[88] LiVecchi A, ACDJAGRPGGRRRGSGSGDHWMCSHS. Powering the blue economy: Exploring opportunities for marine renewable energy in maritime markets. Washington, D.C. https://www.osti.gov/servlets/purl/1525367/; 2019.
[89] Atlantis resources. ltd. AR1500 TIDAL TURBINE. 2016. https://simecatlantis.com/wp-content/uploads/2016/08/AR1500-Brochure-Final-1.pdf. accessed February 1, 2025.
[90] Mcpherson G, Scotland M, Pliatsikas P, Roberts R, Bain N, Queiros J, et al. Marine scotland licence application and Shetland Islands council works license application Shetland Tidal Array extension-environmental assessment Report amendment record revision number date summary of amendments purpose of revision. 2018. www.novainnovation.com [accessed February 17, 2025].
[91] Murray J Orbital O2.2 tidal turbine, EMEC Berth 6, Fall of Warness, Eday, Orkney. Project information document. 2021, February. Orbital Marine Power Limited. https://marine.gov.scot/sites/default/files/project_information_document.pdf [accessed December 19, 2024].
[92] European Marine Energy Centre LTD. Magallanes ATIR Project Environmental Monitoring Plan Document History. 2020. https://tethys.pnnl.gov/sites/default/files/publications/Magallanes-2020.pdf. accessed February 1, 2025.
[93] Hydro A. ANDRITZ HYDRO Hammerfest - renewable energy from tidal currents. https://tethys.pnnl.gov/sites/default/files/publications/Magallanes-2020.pdf. [Accessed 1 February 2025].
[94] Wen Y, Lin P. Exploitation potential of tidal current energy in southern China seas. Energy Convers Manag 2022:267. https://doi.org/10.1016/j.enconman.2022.115901.
[95] James Donegan. ORPC and microgrid inverters background on ORPC. https://tethys.pnnl.gov/sites/default/files/publications/ORPC_Microgrid_presentation_EWTEC_2019_0.pdf. [Accessed 1 February 2025].
[96] Guerra M, Thomson J. Wake measurements from a hydrokinetic river turbine. Renew Energy 2019;139:483–95. https://doi.org/10.1016/j.renene.2019.02.052.
[97] Forbush D, Polagye B, Thomson J, Kilcher L, Donegan J, McEntee J. Performance characterization of a cross-flow hydrokinetic turbine in sheared inflow. Int J Marine Energy 2016;16:150–61. https://doi.org/10.1016/j.ijome.2016.06.001.